Metallurgical Aspects of the Spinning Process in Metallic Liners

S. M. J. Hoseini[1], H. Ghayour[1], A. S. Golazani[1,2]*, M. K. Asgarani[1], I. Ebrahimzadeh[1]

[1]*Advanced Materials Research Center, Department of Materials Engineering, Najafabad Branch, Islamic Azad University, Najafabad, Iran.*
[2]*Department of Materials Engineering, Karaj Branch, Islamic Azad University, Karaj, Iran.*

Abstract

Spinning is one of the novel and unique processes in metal forming for the production of cylindrical and conical thin-walled parts with precise tolerances, good surface smoothness and suitable mechanical properties**.** This process includes conventional spinning, shear forming and flow forming. Metallurgical investigation is great importance in this process. The microstructure obtained from the spinning specimens, especially the shear forming and flow-forming, shows that the grains and the impurity particles are elongated in the direction of the main axis and are also stretched in the circumferential direction. This change in grain size on the roller side was larger than on the mandrel side. Fragmentation of coarse and brittle particles has also been observed. Also, due to the amount of strain and forces applied, the grain size decreases and as a result, the strength increases. The texture of the spinning parts has also changed. As the thickness decreases, the orientation of the grains and textures increases and the large angle boundaries increase.

Keywords: Spinning, Shear Forming, Flow Forming, Microstructure, Texture.

1. Introduction

Spinning is a method of forming metals that has the ability to produce seamless and hollow volumes with a axis of symmetry such as cones, cylinders, tubes, hemispheres or a combination of them. Also in this process, hollow elliptical parts can be produced with special methods. Whereas the deep drawing process cannot be used to produce a part with complex size or structure and the high cost of the tools and mold, spinning is a suitable alternative method. This process is widely used to produce parts needed in the oil and gas industry, automotive, pressure vessels, kitchen appliances, etc. For proper use of these accessories, the final properties of the manufactured part are important. Fig. 1. shows a schematic of the spinning process and the equipment and components of the device [1]. Since the high cost of tools and molds is always an important point in pressing or deep drawing, spinning is an economical and efficient process with many capabilities and an alternative and acceptable method for production of parts.
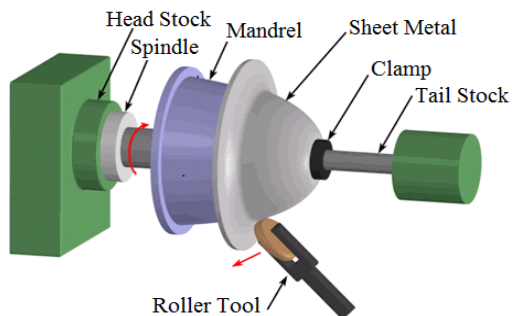

Fig. 1. Schematic of the spinning process [1]

**Corresponding author
Email address: salemiali@kiau.ac.ir*

The advantages of the spinning process are [1, 2, 3]:
- Production without chips, seamless and cold
- Improving the mechanical properties of the material such as yield strength
- Ability to produce parts with different dimensions
- No need for some operations such as machining, grinding, etc.
- It is economical compared to other methods
- Dimensional accuracy of manufactured parts.

The spinning process is divided into two categories in terms of thickness change during shaping: (i) in conventional spinning, the wall-thickness of the blank remains nearly constant throughout the process, thus the final wall-thickness of the spun part is equal to the thickness of the blank and this process can be done with manual and machine equipment. (ii) in shear spinning and flow forming the wall-thickness of the blank is reduced in power spinning or flow forming and can only be done with special equipment [4]. Fig. 2. shows the classification types of spinning process.
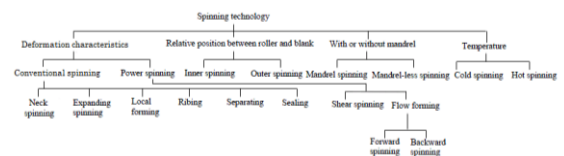

Fig. 2. Classification of spinning processes [5].

1.1. Conventional Spinning

In this method, the deformation is done with a bending mechanism and wall-thickness does not change significantly. This process can be done by using manual or machine devices. In this process, a plate is placed between a rotating mandrel and the

roller of the machine. A compressive force is applied which gradually bends the metal on the mandrel after several working steps [6].

1.2. Shear Spinning

Another type of spinning is shear forming or shear spinning, which is a subset of machine spinning. The reason for this naming is the application of pure shear force that is applied to the workpiece and reduces the thickness and thinning of its wall [6].
In shear spinning, the roller in each pass reduces the workpiece wall-thickness in a predictable and calculable way, while the blank diameter remains constant during the process.
The final thickness of the workpiece in conical shear spinning follows Eq. (1)., which is called the sine law, as shown in Fig. 3. [6, 7].

$$t_f = t_0 \sin\left(\frac{\alpha}{2}\right) \qquad \text{Eq. (1).}$$
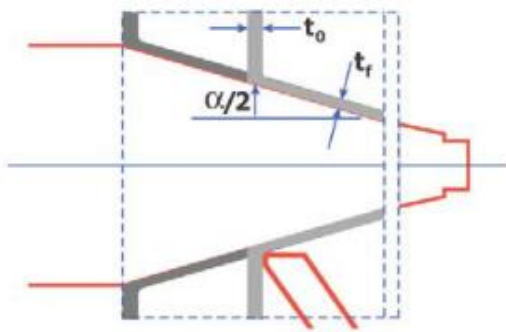$$r = 1 - \sin\left(\frac{\alpha}{2}\right) \qquad \text{Eq. (2).}$$

Fig. 3. Sine law [8].

Where t_f is the final thickness of the workpiece, t_0 is the initial thickness of the preform and ($\alpha / 2$) is the half-angle of the mandrel cone. However, the result is in real condition usually slightly different from what is obtained from the sine law [8].Reduction of the thickness more or less than in Eq. (2). causes the flange to wrinkle or tear. The shear strain γ is obtained from Eq. (3). [9]:

$$\gamma = \cot\left(\frac{\alpha}{2}\right) \qquad \text{Eq. (3).}$$

1.2. Pipe spinning or flow forming

This process is used to make seamless pipe-like parts with high dimensional accuracy.
The preform is tubular and during the process its length increases while the thickness of the tube decreases. Fig. 4. shows a schematic of direct flow forming [8].
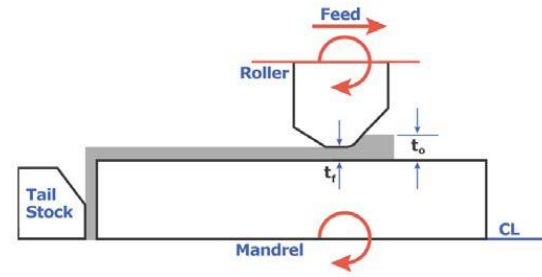

Fig. 4. Schematic of direct flow forming [8].

1.4. Hybrid Spinning

In fact, a combination of conical spinning and tubular spinning occurs in this process. In other words, the spinning process of spherical parts is a combination of shear forming and extrusion [8].
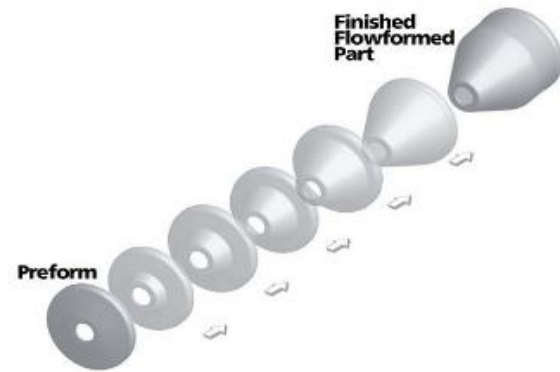Fig. 5. shows the gradual steps in a hybrid spinning.

Fig. 5. Gradual steps in a hybrid spinning [8].

## 1.5. Mechanical Study of Conventional and Shear Spinning Model

Avitzur and Yang [10] in 1960 and Kobayashi [11] in 1961 were the first researchers to identify the spinning process. These two researchers made great efforts to identify forces in the deformation zone. In the deformation zone, they identified three radial, axial, and tangential forces that the tangential force being smaller than the other two forces, while most of the driving force is transmitted through tangential components. In 1985, Held [12] investigated the forces applied during the shear spinning process. In this study, he examined the amount of thickness reduction due to the application of roller pressure on a small path of the disk and provided a method for estimating the forces in the process. Fig. 6. shows the stress distribution in the deformation zone during shear forming. The main deformation region includes tensile stress σ_c and compressive stress σ_m produced by the mold. The bending zone consists of radial compressive stress σ_n and axial shear stress τ_0 produced by the roller. The shear stress τ_0 is perpendicular to the plate [13].
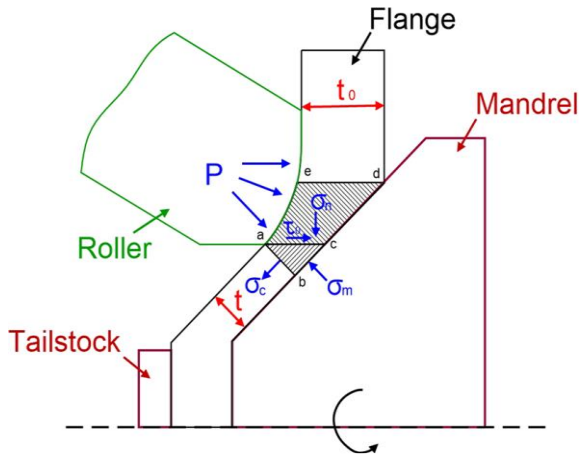
Fig. 6. Schematic of stress state in deformation area during shear spinning [13].

In the conventional spinning model, it is assumed that the thickness will not change during the forming process (as shown in Fig. 7.). To produce the final workpiece with radius R, the initial sheet with radius r is needed. Considering the constant volume and assuming that the thickness is constant for the production of the final part, we follow according to Eq. (4) [14]:

$$\pi r^2 t = \frac{2}{3}\pi[(R+t)^3 - R^3] \qquad \text{Eq. (4).}$$
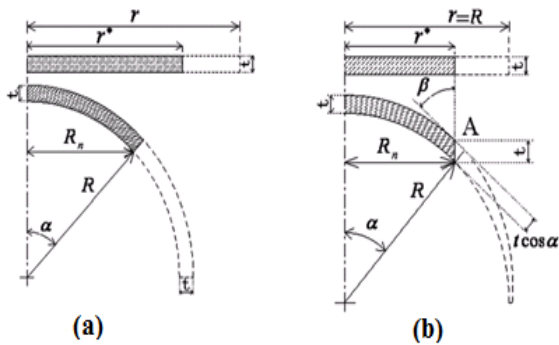
Fig. 7. Theory model of (a) Conventional spinning (constant thickness), (b) Shear forming (constant diameter) [14].

If r* is the radius of the initial sheet required to produce the final workpiece with radius R_n and angle α shown in Fig. 7., with the constant volume theory Eq. (5). is obtained by[14]:

$$\pi r^{*2}t = \frac{2}{3}\pi[((R+t)^3 - R^3)(1 + \cos\alpha)] \qquad \text{Eq. (5).}$$

Where according to Eq. (6). is obtained:

$$\cos\alpha = \frac{\sqrt{R^2 - Rn^2}}{R} \qquad \text{Eq. (6).}$$

Thus we can be expressed r * as a function of R_n according to Eq. (7):

$$r^*(R_n) = \sqrt{\left(2R^2 + 2Rt^2 + \frac{2}{3}t^2\right)\frac{R - \sqrt{R^2 - n^2}}{R}} \qquad \text{Eq. (7).}$$

Due to the fact that in the conventional spinning model there is no change in thickness, so the amount of strain in the direction of thickness will be zero. The engineering hoop strain will easily be obtained as Eq. (8) with consider to the initial $(2\pi r^*)$ and final $(2\pi R_n)$ circumference [14]:

$$\varepsilon_h(R_n) = \frac{2\pi R_n - 2\pi r^*}{2\pi r^*} = \frac{R_n - r^*}{r^*} \qquad \text{Eq. (8).}$$

The engineering radial strain *εr* is determined using constant volume law in terms of the engineering strains as follows

$$(1 + \varepsilon_r)(1 + \varepsilon_h)(1 + \varepsilon_t) = 1 \qquad \text{Eq. (9).}$$
$$\varepsilon_r = \frac{-\varepsilon_h}{1 + \varepsilon_h} \qquad \text{Eq. (10).}$$
$$\varepsilon_r(R_n) = \frac{r^* - R_n}{R_n} \qquad \text{Eq. (11).}$$

In shear spinning model, it is assumed that the diameter of the sheet will not change during the forming process and in fact the thickness in this model will be variable [14]. In this model, the radial position for each element does not change during the process.

Thus the circumference of each circular element $(2\pi R_n)$ remains constant during the process, resulting in zero hoop strain. If t is the initial thickness and α is the angle shown for point A in Fig. 7.b, it can be seen that the final thickness will be equal to t cosα. As a result, engineering strain in the direction of thickness is obtained by Eq. (12) [14]:

$$\varepsilon_t(\alpha) = \frac{t\cos\alpha - t}{t} = \cos\alpha - 1 \qquad \text{Eq. (12).}$$

Therefore, the radial strain is obtained according to the law of constant volume as follows.

$$\varepsilon_t(\alpha) = \frac{1}{\cos\alpha} - 1 \qquad \text{Eq. (13).}$$
$$\varepsilon_t(Rn) = \frac{\sqrt{R^2 - Rn^2}}{R} - 1 \qquad \text{Eq. (14).}$$
$$\varepsilon_t(Rn) = \frac{R}{\sqrt{R^2 - Rn^2}} - 1 \qquad \text{Eq. (15).}$$

1.6. Main spinning parameters

There are three main types of parameters in spinning processes, which are shown in Fig. 8. [15].
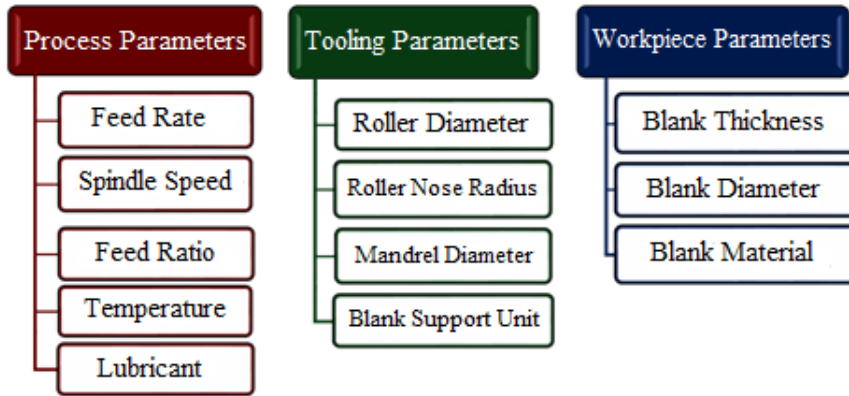
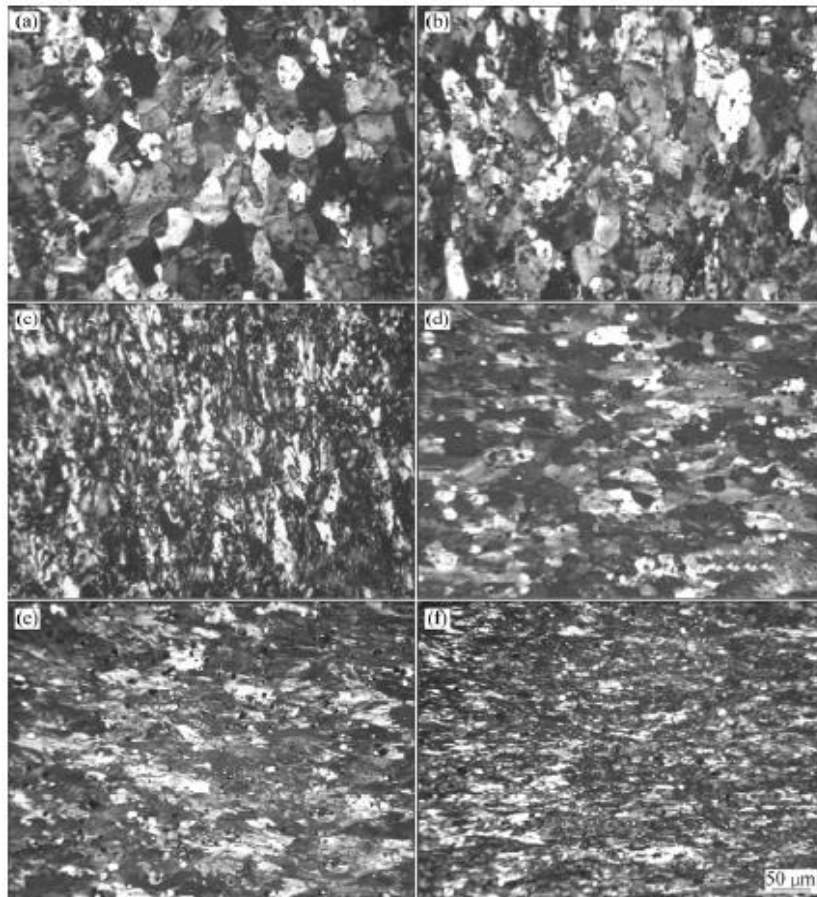Fig. 8. The main parameters of spinning processes [15].

Fig. 9. Influence of strain on microstructure in different planes during shear spinning of AlMg6Mn alloy (a) Reduction=30%, L-T plane; (b) Reduction=50%, L-T plane; (c) Reduction=68%, L-T plane; (d) Reduction=30%, L-S plane; (e) Reduction=50%, L-S plane; (f) Reduction=68%, L-S plane [16].

As we know, microstructure has an important role in controlling the properties of materials. Therefore, it will be very important to pay attention to the influencing factors in the microstructure of the workpiece during the spinning process. In the spinning process, there is little microstructural information and microstructure design, while most of the research presented in this field has been to design mechanical parameters and has been examined more from a mechanical point of view. As a result, the lack of a comprehensive metallurgical investigation in this area is somewhat felt. The main purpose of this study is to investigate the effect of some spinning parameters on microstructure, grain size, texture and finally mechanical properties.

2. Findings
2.1. Shear Spinning

Radovic et al. [16] studied the deformation and microstructure of AlMg6Mn alloy during shear spinning.

They reduced the thicknesses 30%, 50% and 68% by using different mandrels. The grain structure is gradually developed refining during shear spinning. The grains are elongated in the axial direction by increasing the amount of thickness reduction and are also stretched in the rotational direction. In this study, the most optimal combination of strength and elongation was obtained, which has been attributed to grain refinement and reaction of dislocations with Mg and Mn particles and atoms in solid solution. Finally, the effect of initial grain size as well as mechanical properties have been investigated. In this study, they concluded that high accumulated energy, as a result of local deformation and high strain rate, may lead to dynamic recovery. Recovery in Al-Mg alloys usually stops during other deformation modes. On the other hand, using transmission electron microscopy (TEM), it has been proven that dynamic recovery occurs during shear spinning of AlMg3 alloy in high reducing thickness, but this does not occur in cold rolling in the same thickness reduction [16].

They also observed that during shear spinning, grain refinement occurs gradually in both small and large grains as the thickness decreases. The grains are elongated in the axial direction (Fig. 9.a to Fig. 9.c) and also stretched in the direction of rotation (Fig. 9.d to Fig. 9.f). Fragmentation of coarse and brittle particles is also observed. They also reported an important result, they reported that the grain size in the shear spinning specimens did not differ much from the rolled specimens in the same conditions. They reported that shear spinning was effective in improving the strength of AlMg6Mn alloy while maintaining the elongation approximately.

Hardness and tensile strength gradually increase as the wall thickness reductions. This phenomenon is explained by grain refinement, hardening by particle and Mg and Mn effects. Strength and hardness indicate dependence on grain size, which increases with decreasing grain size. High values of elongation are justified by the dynamic recovery that occurs with high accumulation energy as a result of local deformation and high strain rate [16].

Zhan et al. [17] have been studied in 2016 to investigate grain refinement and its mechanism in shear forming, microstructures of aluminum parts that are formed under different deformation conditions, with different deflection ratio (relative to sine law (Eq. (1))). Their results show that after shear spinning, the microstructure is symmetrically distributed around an area of sheet thickness between the inner surface and the center plane (called the neutral area) (Fig. 10.). Electron back scatter diffraction (EBSD) images of these samples are also shown in Fig. 11. Different deflection ratios in shear spinning can lead to grain refinement in different areas along the thickness of the spinning specimen. The nature of the microstructure indicates that the grain refining mechanism is the result of the formation of deformation bands. It has been observed that in deformation bands, the parallel necessary geometric boundaries with the zero deflection ratio are formed and cross GNBs are formed with a positive and negative deflection ratio, which is the result of different stress states affected by different deflection ratios in shear spinning. As a result of the effect of grain refinement, microhardness increases with decreasing deflection ratio (Fig. 12.).
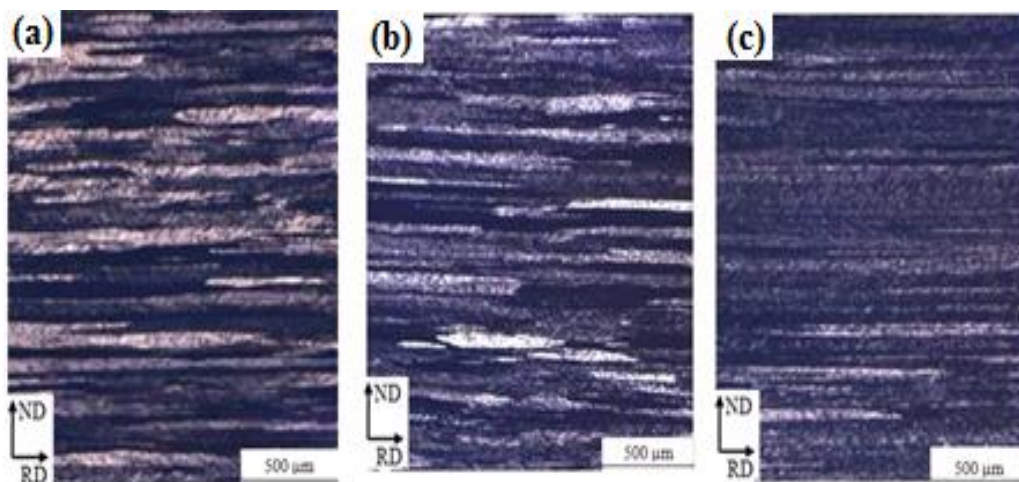

Fig. 10. Microstructure after shear spinning with angle α = 30° in different deflection ratios (a) X = 28.66%, (b) X = 0 and (c) X = -28.33% [17].
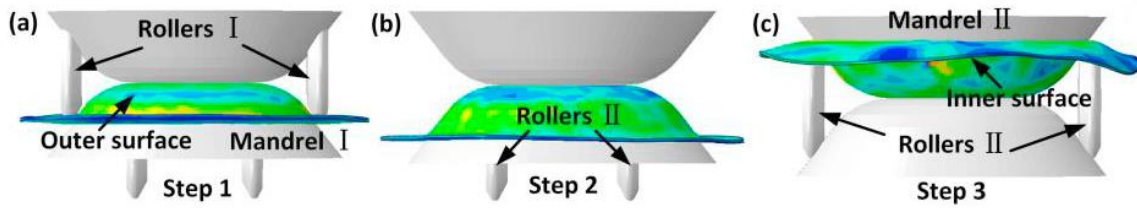
Fig. 13. (a), (b) and (c) schematic of three repetitive shear spinning steps [19].
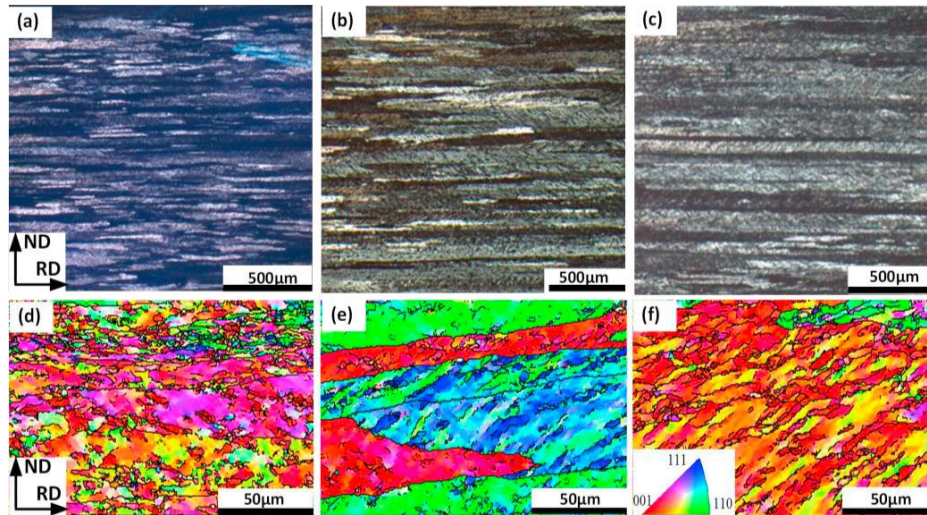

Fig. 14. Optical images in (a) repetitive shear spinning; (b) single-pass shear spinning and (c) two-pass shear spinning; EBSD images in (d) repetitive shear spinning; (e) single-pass shear spinning and (f) two-pass shear spinning [19].
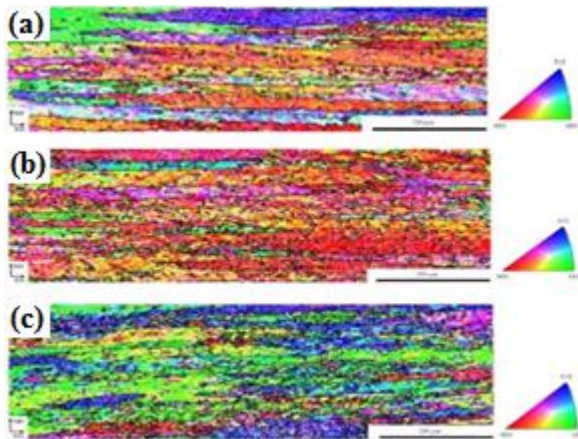

Fig. 11. EBSD images of 3A21-O alloy after shear spinning with angle $\alpha = 30^o$ at (a) X = 28.66% (b) X = 0 and (c) X = -28.33% [17].

Also, according to Brandon et al. [18] research on shear spinning of steel, after deformation, only the solution treatment affects the texture, and the aging treatment alone has no effect on the texture.

Wang et al. [19] used a special spinning technique called repetitive shear spinning. Repetitive shear spinning consists of two successive shear spinning passes along both sides of the sheet metal. Fig. 13. shows a simulation illustrations of this process in three steps using two mandrels. Fig. 14. shows the

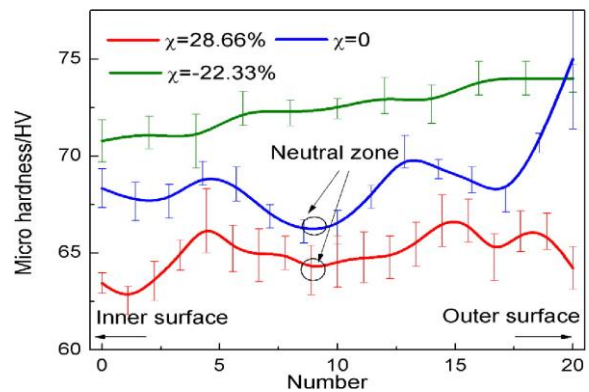microstructures in repetitive, single-pass and two-pass shear spinning.

Fig. 12. Microhardness of the specimen in different deflection ratios obtained at $\alpha = 30^o$ [17].

The microstructure obtained by optical microscopy shows that after shear forming, the grains are elongated in the rollers direction and compressed in the normal direction. Compared to single-pass and two-pass shear spinning, the grains in repetitive shear spinning are more compressed and elongated. Base on the electron back scatter diffraction (EBSD) images, it appears that the grain boundaries in repetitive and two passes shear spinning are formed along the geometrical necessary boundaries (GNBs) to fragment the grains. In repetitive shear spinning,

a large number of small subdivided grains are formed as shown in Fig. 14.d The grain size obtained from the repetitive shear spinning process is smaller than the one-pass and two-pass process [19]. In 2017, Guillot et al. [20] investigated different areas of shear spinning cones from 304L steel as shown in Fig. 15. The raw material with equiaxial grains that becomes a structure with elongated grains after shear spinning. Also, their hardness during the process increases strongly and reaches about 370HV. High local deformation was observed in the form of shear bands along the θ axis of the cylindrical coordinates and slightly titled from the shear forming direction. Microstructural and hardness analysis showed that the homogeneous microstructure is stretched along the shear spinning parts. Transformation of austenite to martensite is observed. The main mechanism of deformation was identified as simple shear. Shear spinning has a significant effect on the microstructure, hardness and texture of the material. In Fig. 15.a shear spinning specimen is divided into five sections from M1 to M5 and tested. Fig. 16. shows the microstructure of the different areas of the deformed sample. Microstructural images are shown and the

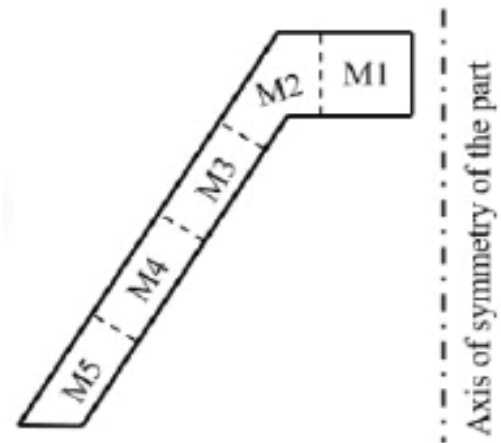initial material called M1 contains some equiaxed grains.

Fig. 15. Test areas [20].

The initial material is heterogeneous and has a relatively weak rolling texture. In the shear spinning areas, M2 to M5 elongated grains are present and only slight microstructural differences are observed. Shear bands that show severe local deformation during plastic deformation are observed [20].
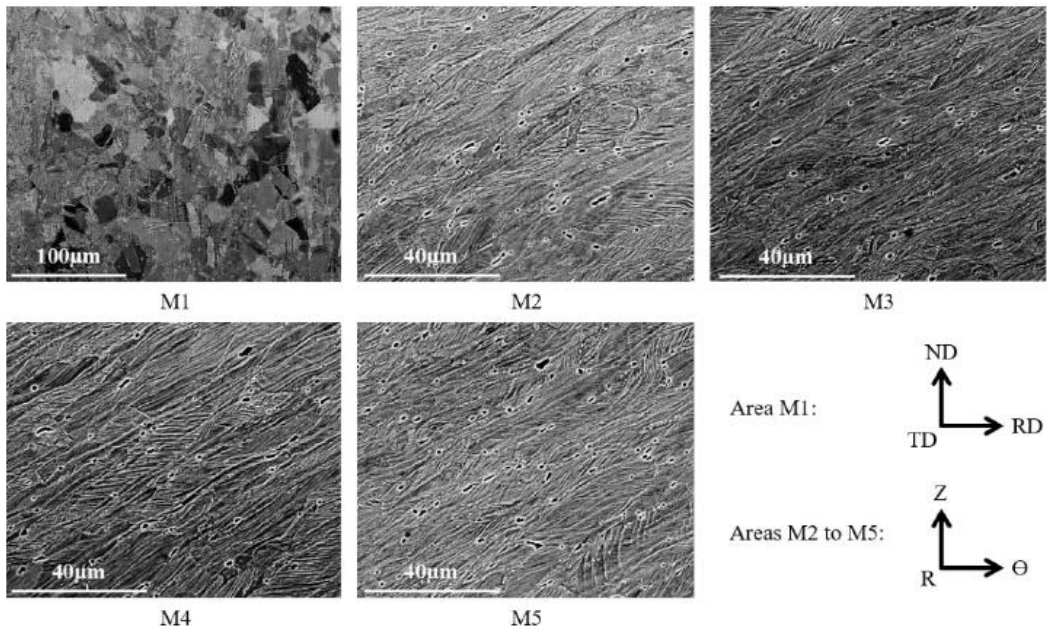

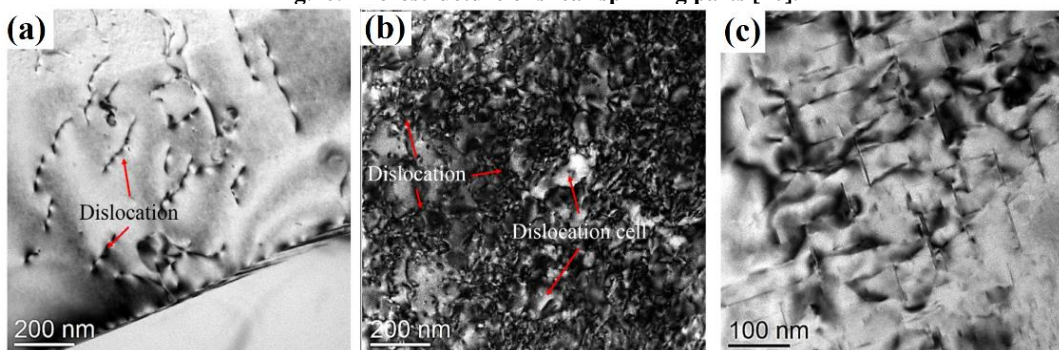Fig.16. Microstructure of shear spinning parts [20].

Fig. 17. TEM images of a) initial sample, b) shear spinning sample with 20% thickness reduction, c) shear spinning sample with 20% thickness reduction and then aged at 175 ° C for 2 hours [22].
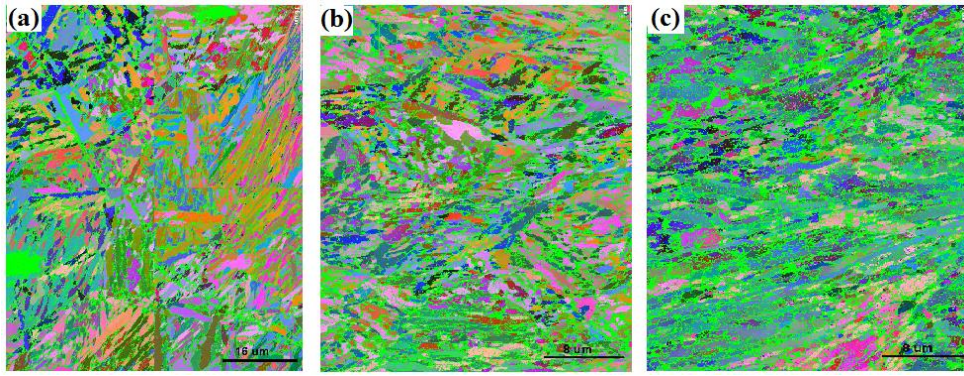
Fig. 18. EBSD analysis image orientation map from a) 0% thickness reduction sample, undeformed sample, b) 30% thickness reduction sample, c) 75% thickness reduction sample [23].
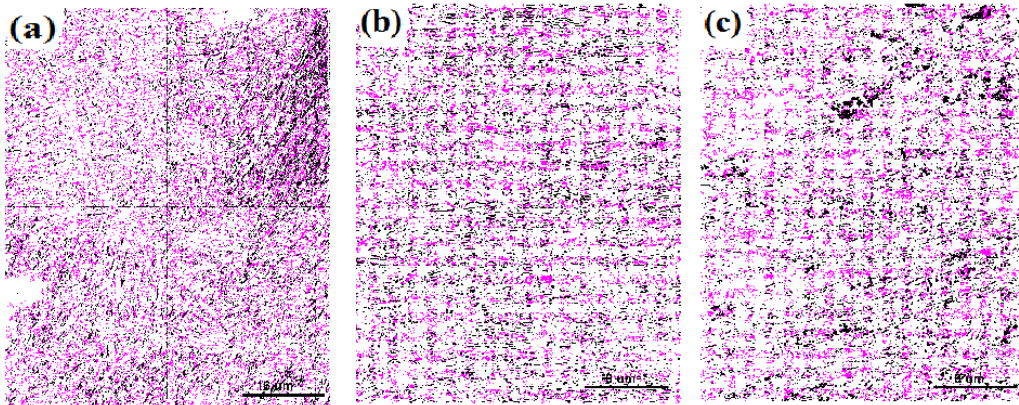

Fig. 19. EBSD analysis of high angle grain boundaries (HAGB) and low angle grain boundaries (LAGB) from from a) 0% thickness reduction sample, undeformed sample, b) 30% thickness reduction sample, c) 75% thickness reduction sample [23].
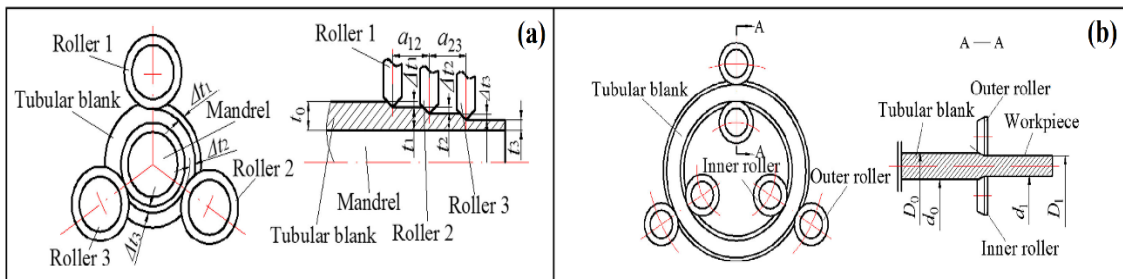

Fig. 20. Principle of (a) stagger spinning and (b) counter-roller spinning [24].

In a study by Valdez et al. [21], based on microstructural and texture analysis, they stated that the main mechanism of deformation in the shear forming process is simple shear, and heavier shear deformation was observed near the roller that lead to formation of finer grains near the roller in the shear formed specimen. Also, these results were successfully agreement with the simulated results.

In 2020, Li et al. [22] investigated the role of the shear spinning process on the aging behavior of AA2219 aluminum alloy. Using transmission electron microscopy (TEM) images shown in Fig. 17., it was found that when the thickness reduction is more than 10%, a large number of dislocation cells and sub-grain boundaries are produced by shear spinning deformation. These dislocation cells and sub-grain boundaries lead to the formation of coarse and non-uniformly distributed precipitates in aging process, which reduces hardness uniformly after aging for more than 2 hours.

2.2. Flow forming

In 2014, Kubialy [23] conducted a study on grain orientation in flow forming. The orientation map of the flow forming area is shown in Fig. 18. The grain orientation in the sample with a 30% reduction in wall-thickness is much more homogeneous than in the undeformed area. The grains are elongated in the direction of deformation, and are not randomly.

Flow forming causes the grains to elongate in the x direction, which results the number of grains decreases in this direction. Fig. 19. shows the high angle and low angle grain boundaries. The ratio (HAGB / LAGB) is equal to (42.56 / 57.44), which indicates a large number of sub-grain boundaries. This indicates that even before the flow forming process, there are sub-boundaries in the microstructure. Kubialy by using EBSD analysis showed that with increasing the amount of strain (reduction of wall-thickness) the orientation of the grains will be much more and more homogeneous and the high angle boundaries will increase somewhat [23].

Xiao et al. [24] investigated the effect of flow forming process on grain refinement and observed the overall grain refinement in the direction of the thickness of the cylinder produced by the spinning method. In this study, they demonstrated the material flow model based on the upper bound method and compared stagger spinning with counter-roller spinning shown in Fig. 20. They also performed metallographic and microstructural analysis, which was very consistent with theoretical analysis.

The microstructure in Fig. 21. shows that the grain refinement in the inner layer was less than the outer layer in stagger spinning. While the percentage of grain refinement in the inner and outer layers in the counter-roller spinning was close to each other [24]. Maj et al. [25] investigated the flow forming of Inconel 718 cylinders. They have reported an enormous increase in tensile strength after cold flow forming.

This huge increase in strength is greater than what is related to the work hardening and dislocations. After heat treatment, a significant decrease in strength has been observed.

They suggested that the aging kinetics and nucleation increase with a large increase in deformation. Very fine precipitations are the result of heat treatment. Large amounts of δ phase in the tested samples have very high strength and maximum elongation. Xia et al [26]. performed several steps of flow forming in ultrafine-grained materials and subsequent recrystallization annealing treatment. The microstructure and mechanical properties of ASTM1020 steel pipe produced by spinning method were investigated. They concluded that a good surface smoothness and an improved spin formability of spun workpiece can be obtained by the process combining of 3 passes spinning followed by a 580 ° C and 0.5 h static recrystallization and 2 passes spinning with a 580 ° C and 1 h static recrystallization annealing under the severe thinning ratio of wall thickness reduction. The grain size of ferrite has strongly decreased after stagger spinning. Fine and equiaxed grains of ferrite were generated through re-nucleation and grain growth by subsequent recrystallization annealing.
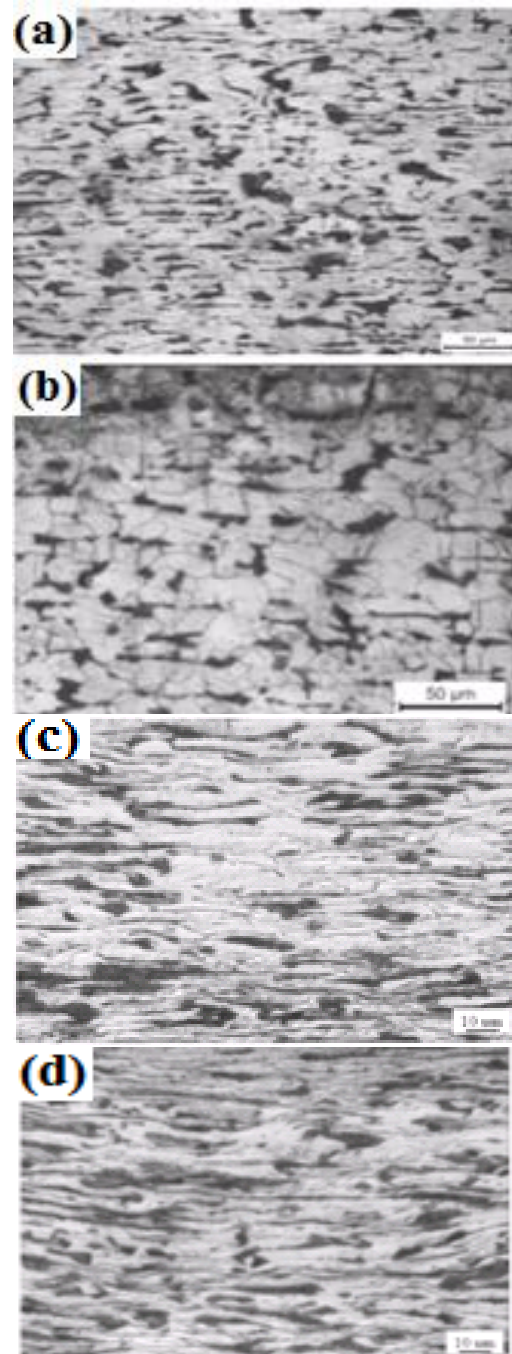
Fig. 21. Microstructure of stagger flow forming sample (a) outer surface, (b) inner surface and flow forming with counter-roller (c) outer surface, (d) inner surface [24].

This research shows that the stagger spinning method has a great potential for making bulk metals with ultrafine grain microstructure. The mechanical properties and microstructure of A356 aluminum under the hot flow forming process have been investigated by Wu et al. [27]. The results of this study showed that the mechanical properties of A356 aluminum alloy were improved and uniform microstructure was obtained. During the hot forming process, Si eutectic particles and Fe-rich phases are dispersed and the porosity is eliminated.
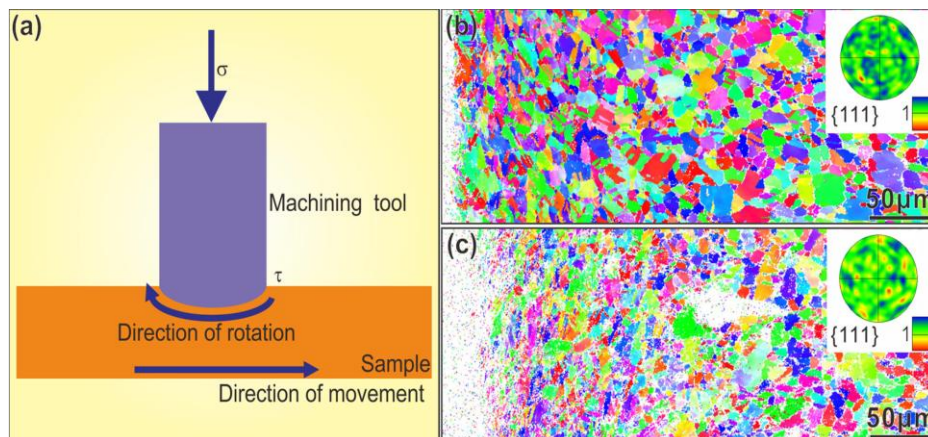
Fig. 22. a) Schematic of the spinning process 3S, b) and c) EBSD images of surface microstructure in samples with two different feed amounts [29].

Recrystallization of Al matrix and AlSiTi phase precipitation also occur. The results of mechanical properties tests also show that an improvement in the final strength, an increase in toughness and a decrease in the microhardness of the deformed sample compared to the cast alloy were observed. These results are attributed to the uniform distribution of fine spherical eutectic Si particles, increase in dislocation density, the elimination of casting defects, and the fine-grained recrystallization grain structure. The microstructure and mechanical properties of hot flow forming and subsequent annealing TA15 alloy pipes were also investigated by Xu et al. [28]. The results of this study showed that with increasing the number of flow forming passes, the fiber microstructure is gradually elongated in the axial direction and the circular microstructure is stretched in the direction of rotation. Also, the tensile stress increases and the elongation decreases not only in the axial direction but also in the circumferential direction. When the thickness reduction ratio increases to close to or over 40%, the tensile strength increases rapidly and the elongation decreases, which means that titanium alloy can be strengthened bi-directionally by power spinning. The ductility of the spun TA15 alloy can be improved by annealing treatment at a temperature not higher than the recrystallization temperature and slightly reducing the tensile strength. Debin et al. [29] tested and investigated the cold flow forming process in Ti-15-3 alloy. They suggested a method that, using reverse extrusion and solution heat treatment, could improve the microstructure of the original billet and prevent cracking during spinning. After the first spinning pass and the solution heat treatment, the crystals of the material are refined and the thickness reduction range increases in subsequent spinning passes. In this way, by increasing the number of spinning passes, the billet is more easily shaped. As the number of spinning passes and the degree of deformation increase, the crystals become more refined.

The maximum allowable thickness reduction rate has increased for each passes and the smallest allowable value for the thickness reduction rate has decreased, which has increased the thickness reduction rate range. As the number of spinning passes increases, spinning will become increasingly easier. Solution Heat treatment is necessary in cold spinning of Ti-15-3 alloy, so that the residual stresses from the deformation are eliminated and the crystals are refined. This treatment will help improve the plasticity of the billet. A new method for surface strengthening was introduced by Ren et al. [30] called surface strengthening by spinning (3S) method, which causes a difference in surface layer microstructure compared to the sub-layers of Cu-11% Al alloy (Fig. 22.).

Depending on the amount of grain refinement, the microstructural difference can be divided into four areas, which include the nanoscale grain area, the fine grain area, the fine grain area, and the coarse grain area from the surface to the center. Meanwhile, the abundance of grain boundaries and twin boundaries has been effective in inhibiting the movement of dislocations in the surface layer during the plastic deformation process. Subsequently, this method has improved the surface mechanical properties due to differences in the surface microstructure compared to the sub-layers.

2.3. Conventional Spinning

In 2020, Gondo et al. [31] conducted research on the conventional spinning in several passes on AA1050 aluminum sheet. By examining the microstructure and texture of the spun workpiece, they showed that the crystalline orientation had changed in two-thirds of the thickness of the workpiece, and included four types of crystalline texture, shown schematically in Fig. 23.
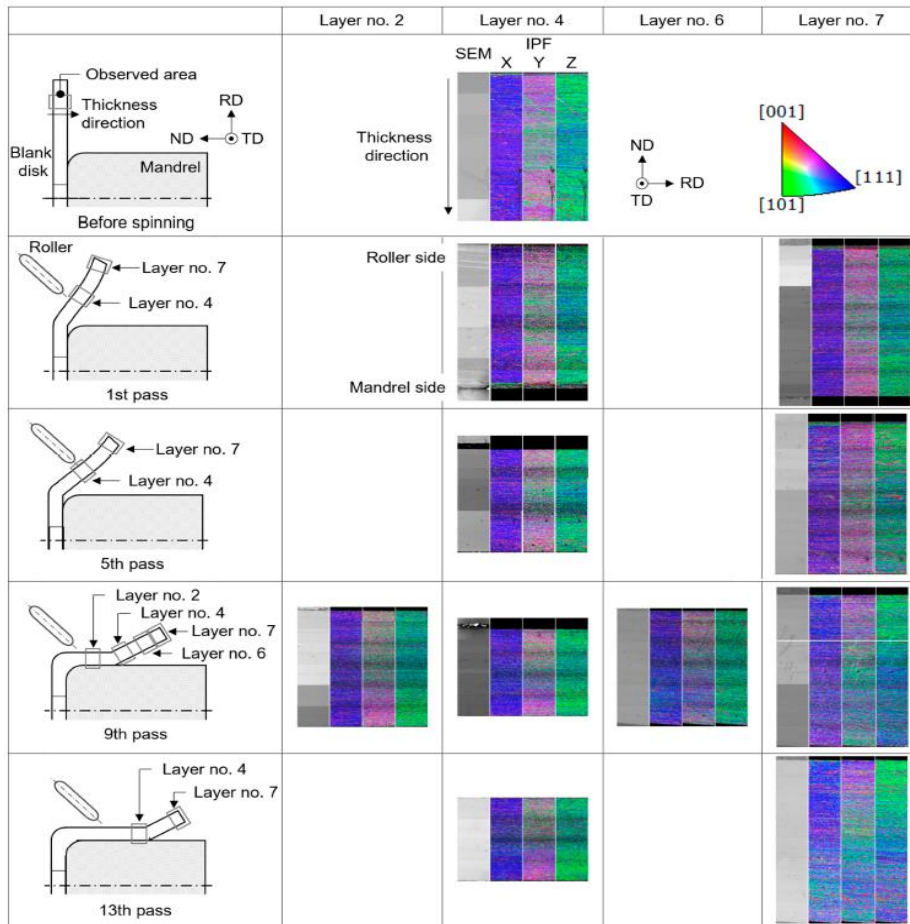
Fig. 24. Distribution of crystal orientation and SEM images along the thickness of spun samples [31].
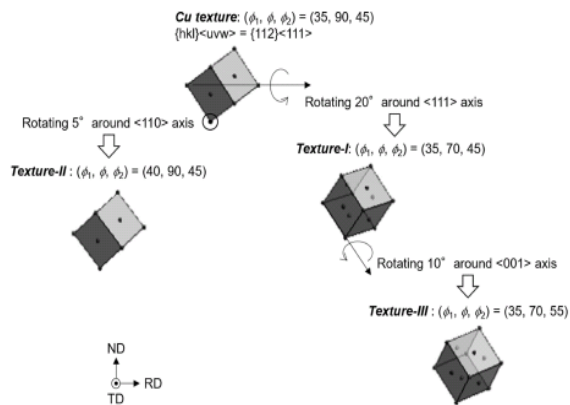

Fig. 23. Relationships among the stable directions: Cu texture, texture-I, texture-II, and texture-III [31].

The Cu texture, "texture-I", which rotated 20° around <111> from the Cu texture; "texture-II", which rotated 5° around its <110> from the Cu texture; and "texture-III", which rotated 10° around its <001> from texture-I. It also shows scanning electron microscopy (SEM) images and IPF maps in the direction of sample thickness in different layers and passes in Fig. 24. The IPF map in the X, Y and Z directions shows the crystal directions which are parallel to the rolling direction (RD), parallel to the normal direction (ND) and parallel to the transverse

direction (TD) of the sheet, respectively [31]. In the IPF maps on the X, Y, and Z planes of the initial disk, there are approximately the same colors in one-third of the thickness. Outer and inner side colors are different. There are similar colors in the IPF map for X direction. The IPF maps in the initial passes were similar to the original disc. In subsequent passes, the colors of the IPF maps on the mandrel side are different from the initial disc. The crystal orientation of the workpiece has changed in two thirds of the thickness from the mandrel side. Therefore, it can be concluded that spinning operations in multiple passes have changed the microstructure, texture and orientation of the grains [31].

3. Conclusion

1. According to the studies, it can be concluded that by performing the spinning process, especially shear spinning and flow forming processes, which have a higher strain and forces on the part, the grain size is reduced and as a result, the strength increases.
2. The microstructure obtained from spinning parts, especially shear spinning and flow-forming, shows that the grains as well as impurity particles have elongated along the main axis and have been stretched in the circumferential direction. This grain

size change was greater on the roller side than on the mandrel side. Fragmentation of coarse and brittle particles is also observed. The nature of the microstructure indicates that the grain refining mechanism is the result of the formation of deformation bands.

3. With the changes in the microstructure, the texture of the spinning parts has also changed. With increasing thickness reduction, the orientation of the grains and texture changes and the high angle boundaries increase.

4. The microstructure of different areas of a cone produced by shear spinning method, from apex to base, has been investigated to show that there is no difference in the microstructure of these areas.

5. The results obtained from hot spinning show that the mechanical properties have been improved and a uniform microstructure is obtained. During the hot forming process, eutectic particles and impurity phases are dispersed and the porosity is eliminated. As the number of passes increases, the fiber microstructure gradually elongated in the axial direction and the circular microstructure stretched in the circumferential direction.

References

[1] P. Pawar, A. Pagar, A. Shah and S. Yevale, Int. J. Recent Innov. Trends Comput. Commun., 5(2017), 1280.

[2] S. Kalpakjian and S. Rajagopal, Appl. Metalworking, 2(1982), 211.

[3] D. Marini, D. Cunningham, P. Xirouchakis and J. Corney, Int. J. Mech. Eng. Technol. (IJMET), 7(2016), 285.

[4] C. C. Wong, T. Dean and J. Lin, International J. Mach. Tools Manuf., 43(2003), 1419.

[5] Q. Xia, G. Xiao, H. Long, X. Cheng and X. Sheng, Int. J. of Mach. Tools Manuf., 85(2014), 100.

[6] E. Hagan and J. Jeswiet, Proc. Inst. Mech. Eng., Part B: J. Eng. Manuf., 217(2003), 213.

[7] W. F. Hosford and R. M. Caddell: Metal Forming Mechanics And Metallurgy, Third Edition, Cambridge University Press, (2007).

[8] M. Sivanandini, S. Dhami and B. Pabla, Int. J. Sci. Eng. Res., 3(2012), 1.

[9] M. Hayama, T. Murota and H. Kudo, Bulletin Of JSME, 8(1965),453.

[10] B. Avitzur and C. T. Yang, Journal of Eng. Ind., Trans. of the ASME, 82(1960), 231.

[11] S. Kobayashi, I. K. Hall and E. G. Thomsen, J. of Eng. Ind., Trans. of the ASME, 83(1961), 485.

[12] M. Held, Propellants, Explosives, Pyrotechnics, 10(1985), 125.

[13] F. Wang, P. Su, L. Qin, S. Dong, Y. Li and j. Dong, Acta Metallurg. Sin., 33(2020), 1226.

[14] H. Beni, Y. Beni and F. Biglari, Part C: J. Mech. Eng. Sci., 225(2010), 509.

[15] M.Tapase, M. han and K.V.Gurav, Int. J. Eng. Dev..Res., 12(2014), 3004.

[16] L. Radović, M. Nikačević and B. Jordović, Trans. Nonferrous Metals Soc. China, 22(2012), 991.

[17] M. Zhan, X. Wang and H. Long, Mater. Des., 108(2016), 207.

[18] D. Brandon, P. Ari gur, Z. Bratt and M. Gur, Mater. Sci. Eng., 44(1980), 185.

[19] X.X.Wang, M.Zhan and M.W.Fu, Procedia. Eng., 207(2017), 1725.

[20] M. Guillot, T. McCormack, M. Tuffs, A. Rosochowsk, S.Halliday and P. Blackwell, Procedia. Eng., 207(2017), 1719.

[21] K. Valdez, B. Wynne and M. Lee, Proceedings Of The 22nd International Esaform Conference On Mater. Forming: Esaform 2019(AIP), 2113(2019), 170001.

[22] Z. Li, M. Zhan, X. Fan, X. Wang and F. Ma, J. Mater. Res. Technol., 9(2020), 4706.

[23] C. Kubilay, Writer, Flow Forming Of Aeroengine Materials. [Performance], PHD Thesis, University of Manchester,En., (2014).

[24] G. Xiao, Q. Xia, X. Cheng and Y. Zhou, The Int. J. Adv. Manuf. Technol., 78(2015), 971.

[25] P.Maj, P.Blyskun, S.Kut, B.Romelczyk-Baishya, T.Morgala, B.Adamczyk-Cieslak and J.Mizera, J. Mater. Proces. Tech., 253(2018), 64.

[26] Q. Xia, G. Xiao, H. Long, X. Cheng and B. Yang, Mater. Des., 59(2014), 516.

[27] X. Y. Wu, H. R. Zhang, H. L. Chen, L. N. Jia and H. Zhang, China Foundry, 14, (2017),138.

[28] W. C. Xu, D. B. Shan, Z. L. Wang, G. P. Yang, Y. LÜ and D. C. Kang, Trans. Nonferrous Metals Soc. of China, 17, (2007), 1205.

[29] S.Debin, L.Yan, L.Ping and X. Yi, J. Mater. Proces. Technol., 115(2001), 380.

[30] C. X. Ren, Q. Wang, Z. J. Zhang, Y. K. Zhu and Z. F. Zhang, Acta. Metallurg. Sin. (En. Lett.), 30, (2017), 212.

[31] S. Gondo, H. Arai, S. Kajino and S. Nakano, Metals, 10, (2020), 793.